Powder Technology 268 (2014) 244–252

Contents lists available at ScienceDirect

Powder Technology

journal homepage: www.elsevier.com/locate/powtec

Determination of elastic properties of particles using single particle compression test

D. Portnikov *, H. Kalman

The Laboratory for Conveying and Handling of Particulate Solids, Department of Mechanical Engineering, Ben-Gurion University of the Negev, Beer Sheva 84105, Israel

ARTICLE INFO

Article history:
Received 19 February 2014
Received in revised form 7 August 2014
Accepted 12 August 2014
Available online 17 August 2014

Keywords:
Single particle compression test
Yield point
Elastic contact stiffness
Effective modulus of elasticity

ABSTRACT

The current work concerns determining elastic properties of particles when employing single particle uniaxial compression tests. These properties are essential for numerical computations using DEM simulations. Five different particulate materials were tested. Three crystalline materials: dead sea salt, potash and green zirconium spheres. Also, two amorphous materials: GNP and glass spheres. The yield point, elastic contact stiffness and effective modulus of elasticity were determined by characterizing the force–displacement experimental curve. Statistical analysis showed that for some materials the effective modulus of elasticity depends on particle size. Finally, a mathematical model was established that describes the distribution of the effective modulus of elasticity and its dependence on the particle size for salt.

1. Introduction

Elastic properties of particles such as Young's modulus and Poisson's ratio are necessary material properties for modeling particle–particle and particle–wall interactions using DEM simulations [1–3]. These properties must be determined experimentally for accurate computational results. Since DEM deals with individual particles, these properties can be achieved only from experiments on single particles.

The contact area caused by compression between a spherical body and a flat surface deforms as a circle. In this case, if the contact surface is rigid and smooth, the force–displacement relationship during elastic deformation is given by [4,5]:

$$F = \frac{4}{3}E^*\sqrt{\frac{d}{2}}\delta^{3/2} \tag{1}$$

where d and E^* are the diameter and the effective modulus of elasticity of the spherical body, respectively. The effective modulus of elasticity is defined as:

$$E^* = \frac{E}{(1-\nu^2)} \tag{2}$$

where E and ν are the Young's modulus and Poisson's ratio of the material. According to Eq. (1), the applied force (F) is linearly dependent on $\delta^{3/2}$, where the effective modulus of elasticity can be found from the slope of this relationship $\left(\frac{4}{3}E^*\sqrt{d/2}\right)$. This dependence also holds for more general cases, where the contact area is elliptical [5].

In a diametric compression test, where a spherical body is subjected to compression between two rigid and flat surfaces, it can be assumed that both sides of the body deform symmetrically. Then Eq. (1) leads to:

$$F = \frac{1}{3}E^*\sqrt{d}\Delta^{3/2} \tag{3}$$

where Δ is the total displacement of the platens ($\Delta = 2\delta$). Following this further, the contact stiffness in the normal direction in the case of elastic deformation can be calculated from the gradient of Eq. (3) as follows:

$$K_{N-el} = \frac{dF}{d\Delta} = \frac{1}{2}E^*\sqrt{d}\Delta^{1/2}. \tag{4}$$

The contact stiffness increases with increase in deformation and particle size and reaches the maximum value in the yield point [6]. Then, the elastic–plastic deformation begins. The force–displacement relationship during elastic–plastic deformation can be derived from the contact stiffness model of Tomas [7] as follows [8]:

$$F = \frac{1}{4}\pi p_Y d\left(1-\frac{1}{3}\sqrt[3]{\frac{\Delta_Y}{\Delta}}\right)\Delta \tag{5}$$

* Corresponding author.
E-mail address: portniko@post.bgu.ac.il (D. Portnikov).

http://dx.doi.org/10.1016/j.powtec.2014.08.011
0032-5910/

where Δ_Y and p_Y are the total displacement and the contact pressure at the yield point, respectively. The contact stiffness during elastic–plastic deformation can be derived then from Eq. (5):

$$K_{N,\ el\text{–}pl} = \frac{dF}{d\Delta} = \frac{1}{4}\pi p_Y d\left(1 - \frac{2}{9}\sqrt[3]{\frac{\Delta_Y}{\Delta}}\right). \quad (6)$$

In the case of elastic–perfectly plastic behavior, the force–displacement relationship beyond the yield point is linearly dependent [9] as follows:

$$F = F_Y + \frac{1}{4}\pi p_Y d(\Delta - \Delta_Y) \quad (7)$$

where F_Y is the yield force. Note, that the contact stiffness is constant during perfectly plastic deformation.

The effective modulus of elasticity of the particle (E^*) can be determined by fitting Eq. (3) to a force–displacement experimental curve within the elastic deformation range [6,10–14], for which the limit of elastic deformation (yield point) must be obtained. In previous studies, Antonyuk et al. [6], Mangwandi et al. [12] and Yap et al. [13] estimated the limit of elastic deformation as the point of deviation from the constant gradient of F^2 versus the Δ^3 plot (see Eq. (3)). Samimi et al. [10] estimated this limit in a similar way, but the Hertzian model was fitted only to the early part (maximum 0.01 N) of the force–displacement data.

This paper focuses on determining the elastic properties of particles using single particle compression tests. An additional method of determining the yield point using contact stiffness plot analysis is also suggested. Moreover, the determined effective modulus of elasticity is represented by a statistical distribution and finally, for the purpose of a DEM simulation, a model which mathematically defines this distribution is proposed.

2. Testing methods and materials

The mechanical behavior of individual particles during compression is measured by using an originally designed and constructed compression tester [15]. According to the principle of the test (Fig. 1), the upper punch, which is operated by a hydro-pneumatic piston, loads the particle at a constant compression force rate until the first breakage appears. The applied force is measured by a Load-Cell with an accuracy of ±0.01% from full scale; and is connected to the lower contact surface. The punch and the lower contact surface are made from alumina 995. The displacement is measured simultaneously by a LVDT sensor with an accuracy of ±5 μm. The tester is able to conduct experiments with individual particles in the size range of 100 μm ÷ 6 mm. All the experiments were conducted with a constant compression force rate of 1 ÷ 2 N/s [15].

Five different materials were tested in the study (Fig. 2). Three crystalline materials: dead sea salt, potash and green zirconium spheres (raw material for zirconium production). Also, two amorphous materials: GNP and glass spheres.

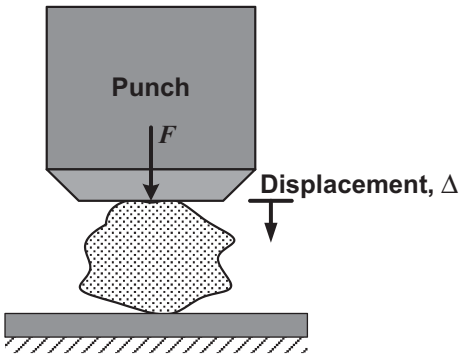

Fig. 1. The principle of a single particle compression test.

3. Experimental results and analysis

3.1. Force–displacement relationship

A typical force–displacement pattern for salt with a narrow particle size interval of 2 ÷ 2.36 mm is presented in Fig. 3. The presented results are of a single experiment. The chart also contains a plot of the calculated contact stiffness. Generally, the graph shows the elastic–plastic behavior of the particle during compression loading until the breakage point (B) which is obtained by a decrease of the measured force.

We can first observe that the curve shape is similar to Hertz model until the yield point (Y), which defines the limit of the elastic deformation. Then, the slope of the curve decreases until the breakage point (B). In order to determine the yield point, the contact stiffness was calculated against the total displacement and is presented in Fig. 3 (right axis). Since the contact stiffness at any point is the gradient of the experimental curve, the calculation was carried out by linear fit of the measured points after dividing the experimental curve into 50 equal sections. It is clear from contact stiffness plot that the elastic contact stiffness increases until a maximum point (Y). Then, elastic–plastic deformation begins and is associated with a moderate decrease of the elastic–plastic contact stiffness until breakage. Since the contact stiffness at the elastic–plastic deformation range is not constant, the deformation of salt particles does not resemble the trend of elastic–perfectly plastic behavior according to Thornton and Ning [9]. The observed behavior resembles an elastic–plastic trend.

Once the yield point is determined, we can check if the elastic deformation of the particle has Hertzian behavior based on Eq. (3). Following this further, Fig. 3 shows the least-square fit within the elastic deformation of the function:

$$F = C_H \Delta^{3/2} \quad (8)$$

where C_H is an empirical constant according to Eq. (3) and depends on the effective modulus of elasticity (E^*) and particle diameter (d). It is clear from Fig. 3 that the elastic deformation of the particle resembles Hertzian behavior meaning that the contact area of the deformable particle has comparatively circular or elliptical geometry. Also, there is a deviation of the experimental curve from the Hertz's model at point Y, which confirms the method of determining the yield point.

Fig. 4 presents the same idea that was shown in Fig. 3 for tests with four different materials (green zirconium, potash, GNP and glass sphere particles). The force–displacement curve, the appropriate Hertz curve and the yield point (Y) were determined by the method described above and presented for each material. According to Fig. 4, we can conclude: the mechanical behavior of green zirconium during the compression until the breakage point is dominant plastic, the behavior of potash is elastic–plastic, the behavior of GNP is dominant elastic and the behavior of glass sphere is elastic without any plastic contact deformation. It is also clear from Fig. 4 that the method of yield point determination is suitable for different materials and can be used as a standard; this method was applied throughout this study.

3.2. Determination of the effective modulus of elasticity

By fitting Eq. (8) to the experimental curve within the elastic deformation as was shown in Figs. 3 and 4, the effective modulus of elasticity of the particle can be determined from the empirical parameter C_H using Eqs. (3) and (8) as follows:

$$E^* = 3C_H/\sqrt{d}. \quad (9)$$